International Journal of Electrical, Electronic and Communication Sciences
ISSN: 2517-9438
Vol:6, No:3, 2012

Stability Issues on an Implemented All-Pass Filter Circuitry

Ákos Pintér, István Dénes

***Abstract*—**The so-called all-pass filter circuits are commonly used in the field of signal processing, control and measurement. Being connected to capacitive loads, these circuits tend to loose their stability; therefore the elaborate analysis of their dynamic behavior is necessary. The compensation methods intending to increase the stability of such circuits are discussed in this paper, including the so-called lead-lag compensation technique being treated in detail. For the dynamic modeling, a two-port network model of the all-pass filter is being derived. The results of the model analysis show, that effective lead-lag compensation can be achieved, alone by the optimization of the circuit parameters; therefore the application of additional electric components are not needed to fulfill the stability requirement.

***Keywords*—**all-pass filter, frequency compensation, stability, linear modeling

I. Introduction

THE all-pass filters are signal processing filters with unity gain signal amplification and adjustable phase delay in their operating range.

Although all-pass filters can be implemented either as analogue or as digital circuits, the digital implementation is always a tradeoff between the signal quality and the hardware performance. If the achievable phase response characteristic is rather simple, the analogue implementation of the all-pass filter can be considered. Basically, there are two implementation manners of realizing such analogue filter circuits. One alternative is the passive implementation, consisting of only passive components like resistors, capacitors and inductors. A number of passive circuit topologies exist, which can be used for this purpose, for instance the Lattice or T-section filters. The other alternative is the active implementation, consisting of active devices like operational amplifiers as well. Through the application of active components, it is possible to omit the bulky and costly inductor components, as well as providing more freedom in the shaping of the filter characteristic.

These circuits are usually used in signal processing systems, especially in audio applications of special sound effects such as the spectral delay filters [8]. Analogue all-pass filters can also be implemented in control or measurement systems, where the phase regulation of a signal is of importance, in order to assure the proper operation of the unit.

Ákos Pintér is with the Mechatronics, Optics and Information Engineering Department, Budapest University of Technology and Economics, Budapest, 1111 Hungary (e-mail: akospinter@gmail.com; akos.pinter@de.bosch.com).

Dr. István Dénes is with the Robert Bosch GmbH, Postbox 1131, Waiblingen, 71301 Germany (e-mail: istvan.denes@de.bosch.com).

II. Operation Principle

A typical configuration of a first-order all-pass filter is shown on Fig. 1. In order to assure the unity gain of the filter, the resistors R connecting to the inverting input of the operational amplifier are chosen with the same resistance value, while the resistor R_c and capacitor C determine the corner frequency of the phase response.

The following equations show the relationship between the input signal and the output signal, considering the operational amplifier as an ideal amplifier, in which the gain and the input impedance are infinite and the output impedance is zero.

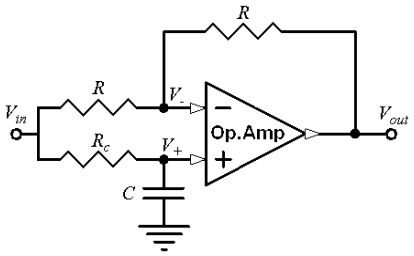

Fig. 1 A first-order all-pass filter

The resistor R_c and the capacitor C connecting serial with each other form a low-pass filter on the non-inverting input of the amplifier, where the voltage is:

$$V_+ = \frac{1}{(j\omega)R_cC+1}V_{in} \tag{1}$$

Using Kirchhoff's junction rule to the inverting input, and considering that the input impedance of the amplifier is infinite, the following equation holds:

$$\frac{V_{in}-V_-}{R} = \frac{V_- - V_{out}}{R} \tag{2}$$

The infinite open loop gain of the amplifier implies that both the inverting and non-inverting inputs are at the same voltage ($V_+ = V_-$). Using this relation, and after multiplying with R and substituting (1) into (2), the equation is:

$$\left(1-\frac{1}{(j\omega)R_cC+1}\right)V_{in} = \left(\frac{1}{(j\omega)R_cC+1}\right)V_{in} - V_{out} \tag{3}$$

After rearranging (3), the transfer function of the input voltage to the output voltage is:

$$H(j\omega)=\frac{V_{out}}{V_{in}}=\frac{1-(j\omega)R_cC}{1+(j\omega)R_cC} \quad (4)$$

After deriving the gain and phase shift information from the transfer function:

$$|H(j\omega)|=1 \quad (5)$$

$$\angle H(j\omega)=-2\arctan(\omega R_cC) \quad (6)$$

As the equations show, the circuit acts in fact as an all-pass filter, since it provides frequency-dependent phase shift with unity gain. The phase response characteristic is similar to that of a two latch element, keeping towards 0 at low frequencies, having a phase shift of -90° at $w=1/R_cC$ and converging towards -180° at high frequencies.

In case of replacing the components R_c and C with each other, the phase response evolves from 180° (low frequencies) towards 0° (high frequencies).

In order to adjust the corner frequency of the filter, a variety of electrically adjustable resistors (e.g. field-effect transistors in "ohmic mode", digitally programmable potentiometers or voltage controlled floating resistors [6]) are available.

III. Frequency Compensation

The frequency compensation is a technique being employed usually in negative feedback amplifier circuits. The main goal for the application of frequency compensation is to avoid the positive feedback of certain frequency domains in the frequency band of the amplifier (with a phase delay of -180° of the feedback signal, the negative feedback changes sign) that causes ringing or the loss of stability of the amplifier.

The general purpose amplifiers are usually compensated internally by adding an integrating capacitance to the gain stage of the amplifier. This capacitor creates a pole with a frequency low enough to reduce the gain to one, at or just below the frequency where the next pole locates, which results in a phase margin of ≈45° depending on the proximity of the further higher poles. This phase margin is usually sufficient to prevent oscillations at the most common feedback configurations, where the amplifier is rather resistively loaded.

However, there are applications, where the operational amplifier has to drive large capacitive loads. The capacitive load acting together with the output impedance brings a new pole into the system. If the capacitance is large enough, the new pole will be located at a frequency lower or just above the cutoff frequency, resulting in a reduced phase margin, which leads to have ringing and stability problems when they are not properly compensated.

Adding new zeros and poles to the system by implementing extra components to the circuit can result in improved stability. There are several compensation methods using this principle, the most of them are discussed in [3]-[5]. The most commonly used method is the so-called dominant-pole or lag compensation method that acts like the internal compensation being discussed formerly, which introduces a new pole in the system. The other conventional methods are the lead compensation, which places a zero in the open loop response to cancel one of the existing poles; the lead-lag compensation placing both a zero and a pole in the open loop response, with the pole usually being at an open loop gain of less then one; and the feed-forward compensation that uses a capacitor to bypass a stage in the amplifier at high frequencies, thereby eliminating the pole that the stage creates.

By choosing the proper compensation technique, some tradeoffs have to be considered, since each technique causes some undesired limitations in the circuit, like the limited output swing, the limited bandwidth, the reduced accuracy or the increased noise sensitivity.

All of the above discussed conventional compensation techniques need additional passive components, however the solution proposed in this paper is based on the parameter tuning of passive components already existing in the circuitry. For such an optimization an accurate model of the system is needed. The derivation of the linear model is discussed in case of a first-order all-pass filter, but can be applied for other feedback amplifier configurations as well.

IV. Linear Modeling of a First-Order All-Pass Filter

A. Two-port network model

At the discussion of the operational principle of the all-pass filter, the ideal operation of the amplifier was assumed. For a more elaborate model analysis the gain and the input impedance of the operational amplifier does not considered to be infinite anymore and the output impedance of the operational amplifier is treated in the model as well.

In order to study the stability of the circuit with respect to the variation of the passive element values, a dynamic model is needed, whereby the characteristic parameters of the feedback can be investigated. The two-port model of the all-pass filter being shown on Fig. 2 divides the whole system into distinct function blocks, such as the input stage (V_{Th}, Z_{Th}) including the input topology as well as the input capacitance of the amplifier, the amplifier (H_{op}), the feedback (H_b) and the output stage (H_{out}) including the load impedance (Z_{load}) and also the output impedance of the amplifier (Z_o). Employing this model, the dynamic behavior of these functional blocks, as well as the characteristic parameters of the feedback loop (e.g. loop gain), together with the behavior of the closed loop can be studied.

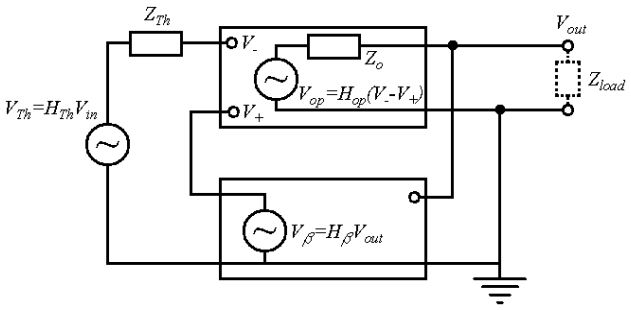

Fig. 2 Series-shunt feedback configuration

There are basically four two-port model configurations that could be employed. The benefit of using the series-shunt configuration is that, the value of the Thevenin equivalent impedance of the input stage (Z_{Th}) can be neglected, since due to the infinite input impedance of the amplifier, no current is flowing through it.

B. Deriving the model parameters

In order to determine the parameters of the two-port model, the operation of the input- and the output stages of the amplifier were separated. After opening the feedback path, the effect of the feedback to the input stage can be replaced with a dependent current source (I_{f*}), depending on the voltage difference between the feedback resistor terminals and on the value of the feedback resistor as shown on Fig. 3 (a). The effect of the feed-forward through the feedback resistor to the output is replaced with the equivalent input network as shown on Fig. 3 (b). In addition, the input capacitance (C_{in}) and the output impedance ($Z_o=sL_o+R_o$) of the operational amplifier are considered in the model as well.

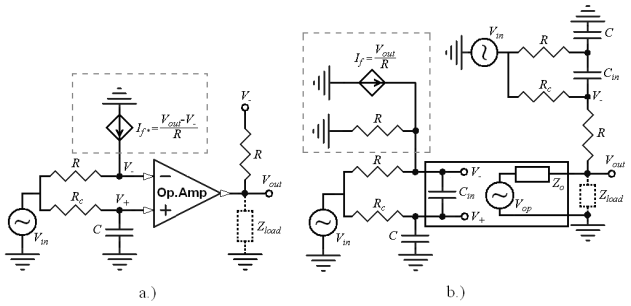

Fig. 3 Equivalent circuit models

The dependent current source I_{f*} marked with the dashed line box on Fig. 3 (a) is equivalent with the dependent current source I_f marked with the dashed line box on Fig. 3 (b). The voltage difference on the input terminals of the operational amplifier ($V_- - V_+$) is a function of V_{in} and V_{out}. The output voltage V_{out} depends further on the amplifier output V_{op} and on the input voltage V_{in} as well (Fig. 3 (b)).

In order to separate and to understand the effect of the feedback and the feed-forward, the block diagram representation of the circuit function is established (Fig. 4).

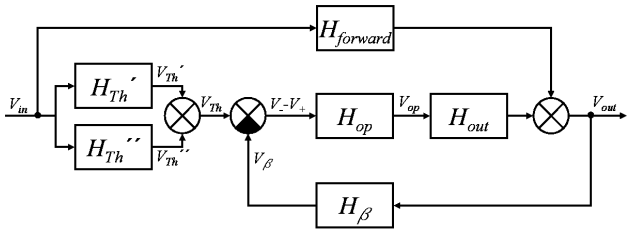

Fig. 4 Block diagram representation of the circuit

The output voltage V_{out} consists of the superposition of the voltages $H_{forward}V_{in}$ and $H_{out}V_{op}$. The effect of V_{in} through the feed-forward branch ($H_{forward}$) can be considered as a disturbance, which is compensated through the feedback branch (H_b). The effect of this disturbance ($V_{dist}=V_{in}$) on the output signal can be calculated as:

$$\frac{V_{out}}{V_{dist}} = \frac{H_{forward}}{H_{op}H_{out}H_\beta} = \frac{H_{forward}}{H_{loop}} \quad (7)$$

Since the feed-forward gain ($H_{forward}$) is significantly smaller then the loop gain of the feedback (H_{loop}), the feed-forward effect of V_{in} can be neglected. The tradeoff through this simplification, on the accuracy of the model behavior can be however observable, if the value of the resistance R is comparable to that of output impedance Z_o, since therewith the gain of $H_{forward}$ becomes bigger. In addition to that, at higher frequencies, where the amplification of the feed-forward ($|H_{forward}|$) is comparable or dominates over the amplification of the feedback loop ($|H_{loop}|$), the model is not valid anymore.

The effect of V_{in} on $V_- - V_+$ (H_{Th}' and H_{Th}'') can be separated from the effect of V_{out} on $V_- - V_+$ (H_b). The transfer functions H_{Th}', H_{Th}'' and H_b are derived with the aid of Fig. 5 (b)(c)(d) respectively, by applying the superposition theorem.

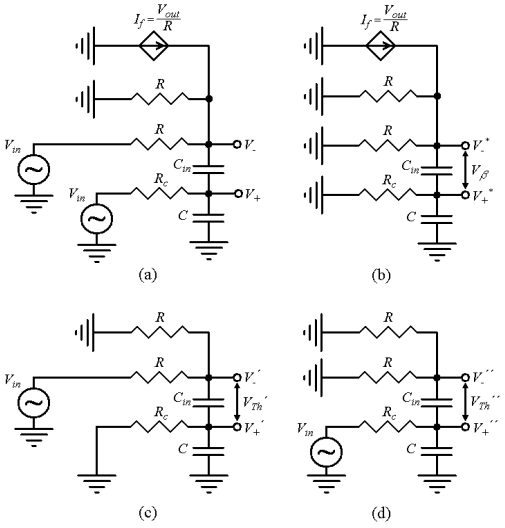

Fig. 5 (a) Equivalent circuit of the input topology
(b) Effect of the feedback current to the amplifier inputs
(c) and (d) Effect of the input voltage to the amplifier inputs

$$V_-' = \frac{R\|\left(Z_{C_{in}} + Z_C\|R_c\right)}{R\|\left(Z_{C_{in}} + Z_C\|R_c\right)+R} V_{in} \quad (8)$$
$$= \frac{j\omega R_c(C_{in}+C)+1}{(j\omega)^2 RR_cC_{in}C + j\omega\left(2R_c(C_{in}+C)+RC_{in}\right)+2} V_{in}$$

$$V_+' = \frac{Z_C\|R_c}{Z_C\|R_c + Z_{C_{in}}} V_-' \quad (9)$$
$$= \frac{j\omega R_cC_{in}}{(j\omega)^2 RR_cC_{in}C + j\omega\left(2R_c(C_{in}+C)+RC_{in}\right)+2} V_{in}$$

$$V_+'' = \frac{Z_C\|\left(Z_{C_{in}} + R\|R\right)}{Z_C\|\left(Z_{C_{in}} + R\|R\right)+R_c} V_{in} \quad (10)$$
$$= \frac{j\omega RC_{in}+2}{(j\omega)^2 RR_cC_{in}C + j\omega\left(2R_c(C_{in}+C)+RC_{in}\right)+2} V_{in}$$

$$V_-'' = \frac{R\|R}{R\|R + Z_{C_{in}}} V_+'' \quad (11)$$
$$= \frac{j\omega RC_{in}}{(j\omega)^2 RR_cC_{in}C + j\omega\left(2R_c(C_{in}+C)+RC_{in}\right)+2} V_{in}$$

After subtracting (9) from (8), the voltage acting on the amplifier inputs to the effect of V_{in} through H_{Th}' can be expressed as:

$$V_{Th}' = V_-' - V_+' = H_{Th}' V_{in} \quad (12)$$
$$= \frac{j\omega R_cC+1}{(j\omega)^2 RR_cC_{in}C + j\omega\left(2R_c(C_{in}+C)+RC_{in}\right)+2} V_{in}$$

After subtracting (10) from (11), the voltage acting on the amplifier inputs to the effect of V_{in} through H_{Th}'' can be obtained as:

$$V_{Th}'' = V_-'' - V_+'' = H_{Th}'' V_{in} \quad (13)$$
$$= \frac{-2}{(j\omega)^2 RR_cC_{in}C + j\omega\left(2R_c(C_{in}+C)+RC_{in}\right)+2} V_{in}$$

After superposing (12) and (13), the Thevenin equivalent voltage source (V_{Th}) is obtained:

$$V_{Th} = V_{Th}' + V_{Th}'' = (H_{Th}' + H_{Th}'')V_{in} = H_{Th}V_{in} \quad (14)$$
$$= \frac{j\omega R_cC-1}{(j\omega)^2 RR_cC_{in}C + j\omega\left(2R_c(C_{in}+C)+RC_{in}\right)+2} V_{in}$$

The effect of V_{out} on V_- -V_+ is represented through H_b, being derived with the aid of Fig. 5 (b):

$$V_-^* = \left(R\|R\right)\|\left(Z_{C_{in}} + Z_C\|R_c\right)I^f \quad (15)$$
$$= \frac{j\omega R_c(C_{in}+C)+1}{(j\omega)^2 RR_cC_{in}C + j\omega\left(2R_c(C_{in}+C)+RC_{in}\right)+2} V_{out}$$

$$V_+^* = \frac{R_c\|Z_C}{R_c\|Z_C + Z_{C_{in}}} V_-^* \quad (16)$$
$$= \frac{j\omega R_cC_{in}}{(j\omega)^2 RR_cC_{in}C + j\omega\left(2R_c(C_{in}+C)+RC_{in}\right)+2} V_{out}$$

After subtracting (16) from (15), the transfer function of the feedback loop (H_b) is expressed:

$$V_\beta = V_-^* - V_+^* = H_\beta V_{out} \quad (17)$$
$$\frac{j\omega R_cC+1}{(j\omega)^2 RR_cC_{in}C + j\omega\left(2R_c(C_{in}+C)+RC_{in}\right)+2} V_{out}$$

In order to obtain the transfer function of the operational amplifier (H_{op}), the gain, the poles and the zeros were taken from a PSpice model as follows. All other parameters of the PSpice model, as the offset and leakage currents of the differential input stage, the large input resistance (1000GW) of the FET inputs, as well as the voltage offset and the common-mode gain are being omitted.

$$H_1 = \frac{1}{\frac{1}{2\pi f_{p1}}(j\omega)+1} \text{ , where } f_{p1} = 274410Hz \quad (18)$$

$$H_2 = \frac{1}{\frac{1}{2\pi f_{p2}}(j\omega)+1} \text{ , where } f_{p2} = 15.9MHz \quad (19)$$

$$H_3 = \frac{\frac{1}{2\pi f_{z3}}(j\omega)+1}{\frac{1}{2\pi f_{p3}}(j\omega)+1} \text{ , where } \begin{matrix} f_{z3} = 2.2MHz \\ f_{p3} = 1.8MHz \end{matrix} \quad (20)$$

$$H_4 = \frac{1}{\frac{1}{2\pi f_{p4}}(j\omega)+1} \text{ , where } f_{p4} = 53MHz \quad (21)$$

$$H_5 = \frac{1}{\frac{1}{2\pi f_{p5}}(j\omega)+1} \text{ , where } f_{p5} = 80MHz \quad (22)$$

$$G = 41 \quad (23)$$

The transfer function of the operational amplifier is:

$$H_{op} = \frac{V_{op}}{(V_+ - V_-)} = GH_1H_2H_3^2H_4^3H_5 \quad (24)$$

The transfer function of the output stage in case of a capacitive load ($Z_{load}=1/(jwC_{load})$) is:

$$H_{out} = \frac{V_{out}}{V_{op}} = \frac{1}{(j\omega)^2 C_{load}L_o + j\omega C_{load}R_o + 1} \quad (25)$$

The open loop gain of the loaded amplifier is:

$$H_A = H_{op}H_{out} = \frac{V_{out}}{(V_+ - V_-)} \tag{26}$$

The loop gain is:

$$H_{loop} = H_A H_\beta \tag{27}$$

The transfer function of the closed loop is:

$$H_{closed} = \frac{V_{out}}{V_{Th}} = \frac{H_A}{1 + H_A H_\beta} \tag{28}$$

The transfer function of the whole system is:

$$H = \frac{V_{out}}{V_{in}} = H_{Th}H_{closed} = H_{Th}\frac{H_A}{1 + H_A H_\beta} \tag{29}$$

V. Verification of the Model

In order to verify the derived linear model, its simulation results were compared to the simulation results of the numerical PSpice model of the circuit.

On Fig. 6, the linear model and the PSpice model of the filter circuit without the feedback resistor *R* were compared to each other. The displayed transfer function of the overall system after opening the feedback path is $H_{Th}H_{op}H_{out}$ as can be seen on Fig. 4.

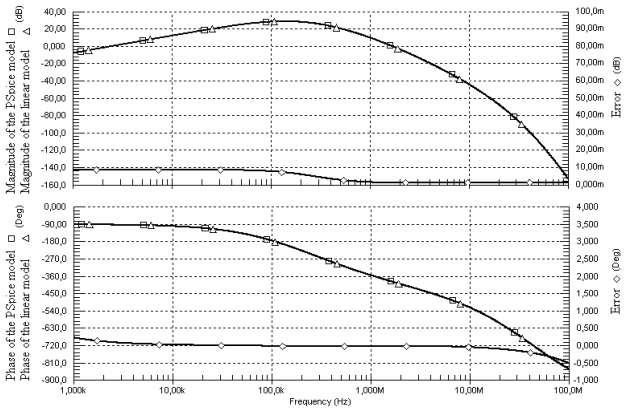

Fig. 6 Transfer functions of the open loop gain

The gain and phase values of the corresponding transfer functions are shown on the left axis, while the error between the models is presented on the right axis. The most significant error in the magnitude of the open loop gain is less then $9 \cdot 10^{-3}$ dB in the relevant frequency range, which means less then 0.11% voltage difference between the output signals, while the most significant phase difference is also less then 0.5 degree.

Fig. 7 shows the transfer functions of the all-pass filter (*H*) being loaded with a 10 nF capacitor. The non-linear behavior - being neglected in the model - is causing deviations at the main corner frequency compared to the simulation result. At higher frequencies, the assumption ($|H_{forward}| << |H_{op}H_{out}H_b|$) does not hold, being the main reason for the differences at the frequency plots at this frequency domain. However in the operating range, the error by means of magnitude is less then 1dB and by means of phase is less then 10 degree.

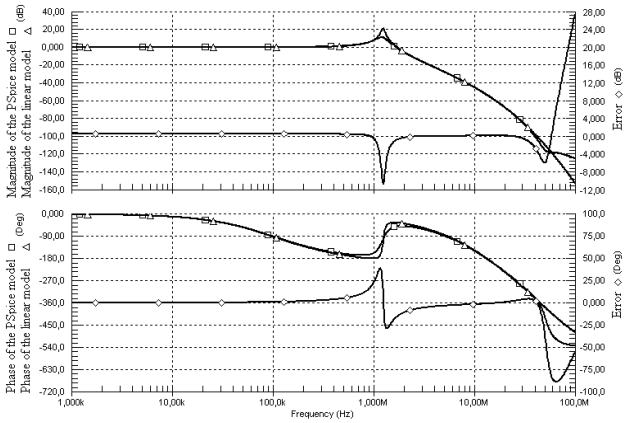

Fig. 7 Transfer function of the whole system

VI. The Effect of the Parameter Variation on the Stability of the Filter

Using the linear model of the circuit, the effect of the capacitive load on the open loop transfer function (H_A) is shown on Fig. 8. The frequency plots of the unloaded open loop gain, the modified open loop gain and the inverse transfer function of the feedback loop are displayed. Due to the new pole being introduced through the load capacitance in the open loop function, the $1/H_b$ curve intersects the modified open loop curve at a slope (rate-of-closure) of more then 40 dB/decade. Since the frequency of the intersection is the cutoff frequency of the loop gain, this means that the phase margin of the capacitive load case is negative (Φ_m=-5.43°, the phase margin without any load is Φ_m=30.98°), which results in an instable system.

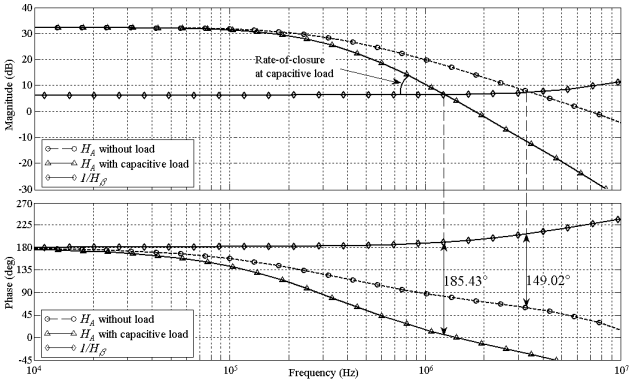

Fig. 8 Effect of the capacitive load to open loop gain

Considering that the condition $|H|=1$ must hold through the whole operating range and the corner frequency ($w=1/R_cC$) of the filter must remain unchanged, there are two alternatives to

modify the dynamic properties of the all-pass filter. One possibility is to change the value of the parameter R and leave the other parameters (R_c, C) unchanged. The other one is to alter the parameters R_c and C, in a way that the impedance ratio of them remain unaffected ($Z_{Rc}/Z_C=1/R_cC=constant$), while the parameter R remain unchanged as well.

Fig. 9 (a) shows the effect of the varying R on the elements of the loop gain (H_A and H_b). On the figure, the magnitudes of the loaded open loop response (H_A) and of the inverse feedback loop response ($1/H_b$) are shown to the case of different resistor values of R. The variation of resistance R – as it can be seen from (25) - does not affect the open loop response at all, however, it has a significant effect to the feedback loop (H_b). By increasing the resistance R, the frequency of one of the two poles of the feedback loop decreases, and respectively, by decreasing R the frequency of this pole increases. Since it would be difficult to obtain the rate-of-closure values on the upper diagram and thereby to get information about the stability, a zero-pole map containing the dominant poles of the whole system (H) as a function of R is displayed on Fig. 9 (b).

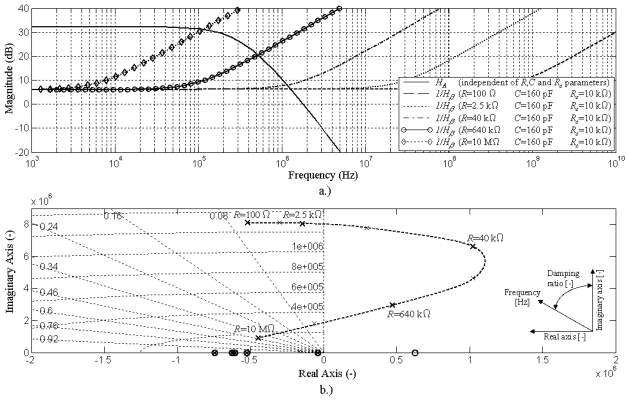

Fig. 9 The effect of varying parameter R

As the zero-pole map shows, the unstable region of the diagram can be left either by increasing or by decreasing the value of R, however at lower R values, the phase margin is rather small, since after a while the increasing of the pole frequency does not affect the rate-of-closure. A more effective way to increase the phase margin is to select higher R values. However the using of large resistances results in increased amount of thermal noise and it reduces strongly the bandwidth of the filter as well.

Fig. 10 shows the effect of modifying the parameters R_c and C. As it can be seen from (25), the variation of these parameters does not affect the open loop response (H_A), however, it does have a significant effect on the feedback loop characteristics (H_b). By keeping the corner frequency ($w=1/R_cC$) constant, and decreasing the capacitance value C, the resistance R_c can be determined. As the capacitance value decreases, the 2 poles of the feedback loop are repelling from each other, leaving the zero of the transfer function at its original place. As Fig. 10 (b) shows, the decreasing of the capacitance C leads to a better stability.

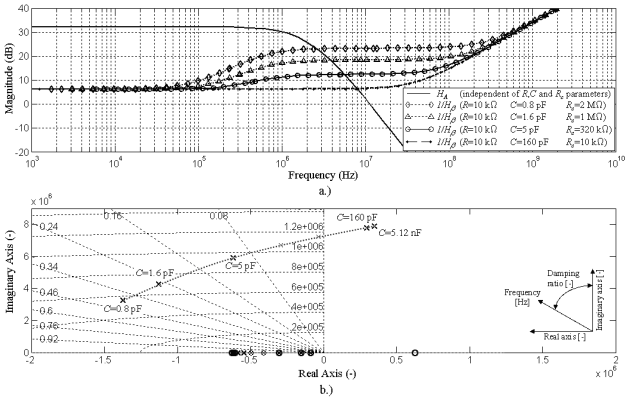

Fig. 10 The effect of varying parameters C and R_c

In order to plot the effect of the variation of the two independent variables R and C, the application of a zero-pole map with polar coordinates is more suitable. In the polar coordinate system, the radius represents the natural frequency of the conjugate pole pairs, while the angle of the radius and the imaginary axis (f) is a non-linear function of the damping factor ($z=\arcsin(f)$) of the corresponding conjugate pole pair, which is a good mathematical indicator of the stability of a system. For $0<z<0.7$ the phase margin can be estimated with the linear relation of $F_m=100z$.

Fig. 11 shows the stability map for the parameter optimization, where the contour lines of the different resistor values of R are signed with a single-dotted line, while the double-dotted lines indicate the changes in the capacitance values of C (R_c).

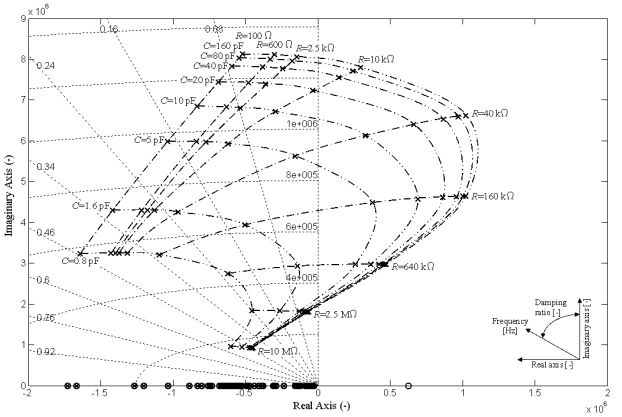

Fig. 11 Pole-Zero map of the parameter change

As it can be seen, different options exist to improve the stability of such circuit. In case of large R resistance values, stability can be achieved, however the frequency band of the closed-loop system is strongly deteriorated. On the other hand these large R resistance values make the system rather insensible to C (R_c) parameter changes. By decreasing the C capacitance and R resistance values the stability can be

reached as well, having even the advantage of a larger bandwidth of the closed-loop system.

Fig. 12 shows the transfer functions of the all-pass filter (*H*) with three different parameter sets. The system is being stabilized by applying a high *R* resistance value (doted line) and also by applying a small *R* resistance and a small *C* capacitance value (dashed line). The third characteristic refers to an unstable system (continuous line).

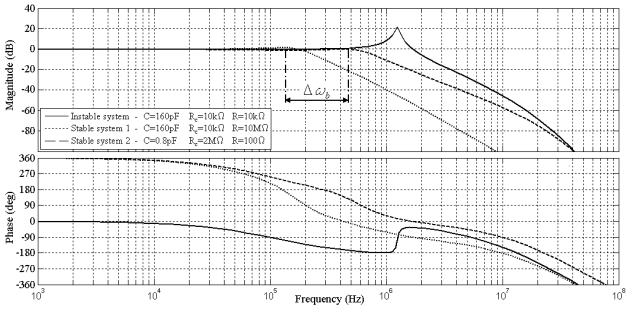

Fig. 12 The closed loop of the stabilized system

As Fig. 11 shows, both stabilization manners cause an increased damping ratio of about 0.45 (resulting in a phase margin of around 62°), however, in case of compensating through large *R* values, a significant decrease in the bandwidth (Δw_b) is occurred (Fig. 12).

Based on the simulation results of the linear model, a significant filter stability improvement can be achieved through decreasing the values *R* and *C* (accordingly by increasing the resistance R_c), however it is recommended to validate these results through the non-linear simulation models, in order to investigate the effect of the non-linear behavior of the operational amplifier, and the effect of the feed-forward character of $H_{forward}$ as well.

For the initial design of the circuit, the second order analytic model of the operational amplifier can be used, however, in this case, in order to confirm the dynamic behavior of the final configuration, the application of a numerical model of the circuit is strongly recommended.

This compensation technique is similar to the so-called lead-lag (or noise gain) compensation treated in [4], with the exception that in our compensation no additional electric components are being used. The advantage of the lead-lag type compensation is that it reduces neither the output swing nor the accuracy of the filter, and it affects just slightly the bandwidth of the system. The increased noise sensitivity however has to be considered in a noisy environment or in noise sensitive circuits.

VII. Conclusion

As the results of the simulation show, it is possible to achieve a significant improvement of the stability, only by optimizing the passive components already existing in the circuit. Through the simplification of the electric circuitry by omitting the additional electric components, the overall reliability of the implemented all-pass filter can be increased, by reducing the space requirements and by cutting on the production costs on the same time.

References

[1] Paul R. Gray and Robert G. Meyer, Analysis and Design of Analog Integrated Circuits. New York: John Wiley & Sons, Inc, 1993.
[2] U. Tietze and Ch. Schenk, Electronic Circuits: Handbook for Design and Application. Berlin: Springer, 2008.
[3] Kumen Blake “Driving capacitive loads with Op Amps” Microchip Application Note 884.
[4] Tim Green “Operational Amplifier Stability – Part 6” Texas Instruments Design Reference
[5] “Operational amplifier stability compensation methods for capacitive loading applied to TS507”ST Microelectronic Application note AN2653.
[6] Bhaba Priyo Das, Neville Watson and Yonghe Liu “Simulation of Voltage Controlled Tunable All Pass Filter using LM13700 OTA” International Journal of Electrical and Information Engineering 4:4, 2010.
[7] Julius O. Smith III, Physical Audio Signal Processing. W3K Publishing, 2010, ISBN 978-0-9745607-2-4.
[8] Jussi Pekonen and Vesa Välimäki “Spectral delay filters with feedback and time-varying coefficients” Proc. of the 12th Int. Conference on Digital Audio Effects (DAFx-09), Como, Italy, September 1-4, 2009M. Young, *The Techincal Writers Handbook.* Mill Valley, CA: University Science, 1989.